NOTES AND CORRESPONDENCE

Is the Mass Sink Due to Precipitation Negligible?

CHONG-JIAN QIU

Cooperative Institute for Mesoscale Meteorological Studies, University of Oklahoma, National Oceanic and Atmospheric Administration, Norman, Oklahoma

JIAN-WEN BAO

Department of Meteorology, The Pennsylvania State University, University Park, Pennsylvania

QIN XU

Cooperative Institute for Mesoscale Meteorological Studies, University of Oklahoma, National Oceanic and Atmospheric Administration, Norman, Oklahoma

3 October 1991 and 18 June 1992

ABSTRACT

The significance of mass sinks (or sources) due to precipitation (or evaporation) is examined using numerical experiments performed with the Pennsylvania State University–National Center for Atmospheric Research Mesoscale Model. The results show that the effect of mass sinks (or sources) can have a significant impact on numerical simulations of heavy precipitation. When this effect is ignored, as is commonly done in most global and regional weather prediction models, precipitation is reduced in the model.

1. Introduction

The mass sink (or source) due to precipitation (or evaporation) has been neglected in almost all the meteorological numerical models. This approximation has commonly been accepted as good, but has recently been questioned by Trenberth et al. (1987) and Gu and Qian (1991). The depletion of water substance due to condensation and precipitation may cause a significant decrease in mass of the moist air, while the evaporation of water substance from the ground into the atmosphere may increase the mass of the moist air. These two processes of water substance transport are not even globally balanced on the climatic time scale. In particular, Trenberth et al. (1987) and Van den Dool and Saha (1993) showed that the contribution of water vapor to surface pressure makes the global mean mass vary annually by about 0.3–0.5 mb. The imbalance between the mass of precipitation and evaporation generally increases as the spatial scale goes down from global to regional or smaller scales. In a heavy-precipitation event, the local depletion of water substance due to condensation and precipitation can be much larger than the replenishment of water substance due to surface evaporation, so the resultant mass sink can be significant. The local dynamical significance of the mass sink (or source) due to precipitation (or evaporation) was first presented for consideration and tested by Gu and Qian (1991) with a coarse-resolution numerical model (six vertical levels). Their formulations neglected the effect of mass sinks (or sources) on momentum and thermal fluxes [i.e., the right-hand-side terms in (3.1)]. It is desirable to further examine this problem with a more complete formulation of the mass sink (or source). Toward this end, numerical experiments are performed with the Pennsylvania State University (PSU)–National Center for Atmospheric Research (NCAR) Mesoscale Model to examine the quantitative aspect of the above problem.

2. Continuity equation of moist air

Let us consider a system composed of dry air of density ρ_d, water vapor of density ρ_v, and water condensate of density ρ_w. The total density is $\rho = (M_d + M_v + M_w)(V_a + V_w)^{-1} \approx \rho_d + \rho_v + \rho_w$, where M_d is the mass of dry air, M_v the mass of water vapor, M_w the mass of water condensate, and V_a and V_w the volumes of moist air and water condensate, respectively. The mass continuity equations for the three ingredients are

Corresponding author address: Dr. Qin Xu, Cooperative Institute for Mesoscale Meteorological Studies, University of Oklahoma, National Oceanic and Atmospheric Administration, 100 East Boyd, Room 1110, Norman, OK 73019.

$$\partial_t \rho_d + \nabla \cdot (\rho_d \mathbf{v}) = F_d, \quad (2.1)$$

$$\partial_t \rho_v + \nabla \cdot (\rho_v \mathbf{v}) = S_{ev} - S_{con} + F_v, \quad \text{and} \quad (2.2)$$

$$\partial_t \rho_w + \nabla \cdot [\rho_w (\mathbf{v} - \mathbf{v}_r)] = S_{con} - S_{ev} + F_w, \quad (2.3)$$

where S_{ev} is the evaporation rate of water condensate, S_{con} the condensation rate of water vapor; F_d, F_v, and F_w represent the effects of diffusion; $\mathbf{v}_r$ is the velocity of water condensate relative to air; and $\nabla \equiv (\partial_x, \partial_y, \partial_z)$. The mass continuity equation for the total density is given by the sum of (2.1)–(2.3):

$$\partial_t \rho + \nabla \cdot (\rho \mathbf{v}) = F - S_r, \quad (2.4)$$

where $F \equiv F_d + F_v + F_w$, and

$$S_r \equiv -\nabla \cdot (\rho_w \mathbf{v}_r) \quad (2.5)$$

is the generation rate (due to flux convergence) of precipitation per unit air mass.

In the σ coordinates the above mass continuity equation (2.4) takes the following form:

$$\partial_t \pi + \nabla_H \cdot (\pi \mathbf{v}_H) + \frac{\partial(\pi\omega)}{\partial\sigma} = \frac{g\partial(\rho_w \mathbf{k} \cdot \mathbf{v}_r)}{\partial\sigma} + \pi \frac{[F - \nabla_H \cdot (\rho_w \mathbf{v}_r)]}{\rho} \equiv S, \quad (2.6)$$

where $\sigma \equiv (p - p_{top})/\pi$ and $\pi \equiv p_{sfc} - p_{top}$; $\nabla_H \equiv (\partial_x, \partial_y)$; $\mathbf{v}_H \equiv (u, v)$; $\omega \equiv d\sigma/dt$; $\mathbf{k}$ is the vertical unit vector; and S is the mass sink–source term, or MSS term for short. Since only the hydrostatic approximation is used in the derivation of (2.6), the MSS term can be very accurate provided the density ρ_w and velocity $\mathbf{v}_r$ (relative to air) of water condensate can be precisely computed. In most numerical models (such as the one used in this paper), however, water condensates are assumed to fall immediately to the ground as soon as they form. In this case, $S_r \approx g\partial(\rho_w \mathbf{k} \cdot \mathbf{v}_r)/\partial\sigma$ is simply the condensation rate. This may cause some errors in the computation of the MSS term. Neglecting the horizontal diffusion terms and integrating (2.6) vertically give the surface pressure tendency equation

$$\partial_t \pi + \int_0^1 \nabla_H \cdot (\pi \mathbf{v}_H) d\sigma = g(E_s - P_r), \quad (2.7)$$

where E_s is the evaporation rate and $P_r = (\rho_w \mathbf{k} \cdot \mathbf{v}_r)|_{\sigma=1}$ is precipitation rate at the surface. Equation (2.7) includes the contribution of surface evaporation and precipitation, which is similar to Eq. (5) of Trenberth (1991). According to Trenberth, "this equation is more accurate than commonly used in meteorology where the right-hand side is typically ignored." Typical values for $E_s - P_r$ are ± 5 mm day^{-1} in the tropics and subtropics, resulting in an equivalent surface pressure tendency of 0.49 mb day^{-1} (5.5×10^{-4} Pa s^{-1}), which is one-tenth of the typical value of the total pressure tendency. This contribution is not negligible in an advanced numerical model. In heavy-precipitation events, rainfall rates can easily exceed 10.0 cm day^{-1} (or 5 mm h^{-1}), which can be much larger than the surface evaporation rates. The resultant contribution to the surface pressure tendency could be as large as 10 mb day^{-1}. It may be speculated further that the mass depletion due to precipitation tends to reduce the surface pressure, which may in turn enhance the low-level moisture convergence and give a positive feedback to precipitation. Thus, neglecting the MSS term may cause precipitation to be underpredicted in the model. However, it is difficult to tell how much error is due directly to the neglected MSS term as initial MSS-related errors may grow with time.

3. Numerical experiments

The PSU–NCAR model described by Anthes et al. (1987) is used to investigate the impact of the MSS term in (2.6) on the regional forecasts of heavy precipitation. The computational domain contains an array of 46×61 grid points, spaced approximately 80 km apart. The vertical dimension is resolved by 16σ levels, including 5 levels in the "high-resolution" PBL. Since the horizontal resolution is relatively coarse, the Kuo–Anthes scheme of cumulus parameterization is selected for our numerical experiments. The excess water vapor over a critical relative humidity is removed as precipitation, while evaporation in unsaturated layers is not allowed. Since the flux forms of the momentum and thermodynamic equations were derived in the PSU–NCAR model by using the mass continuity equation and ignoring the MSS term in (2.6), recovering the MSS term in (2.6) brings a new (vector) term in the (vector) flux form of the momentum and thermodynamic equations:

$$\partial_t(\pi \mathbf{a}) + (\text{other terms}) = \pi \mathbf{a} S, \quad (3.1)$$

where $\mathbf{a} \equiv (u, v, T)$ and S is the MSS term defined in (2.6). The vertical velocity is computed by the following vertical integration of (2.6):

$$\omega = -\frac{1}{\pi} \int_0^\sigma [\partial_t \pi + \nabla_H \cdot (\pi \mathbf{v}_H) - S] d\sigma. \quad (3.2)$$

Again, we may call all S-related terms in (2.6)–(3.2) the mass sink–source terms, or MSS terms.

By using the same initial field obtained from the National Meteorological Center (NMC) analysis data at 0000 UTC 22 November 1983, two comparative runs are performed for 36 h with the standard and modified (MSS terms added) PSU–NCAR models, which are referred to as the standard run and MSS run, respectively. During this period, a cyclone formed in the central United States and moved northeastward. Precipitation occurred over a large area of the eastern United States and the maximum accumulated precipitation exceeded 10.0 cm in the central region of precipitation.

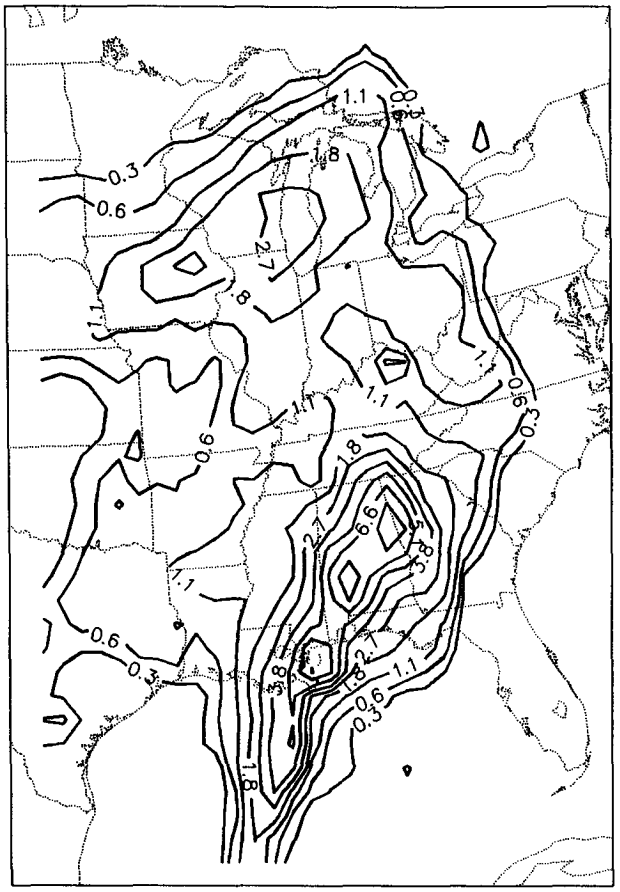

FIG 1. Thirty-six-hour precipitation forecast (cm) by standard run.

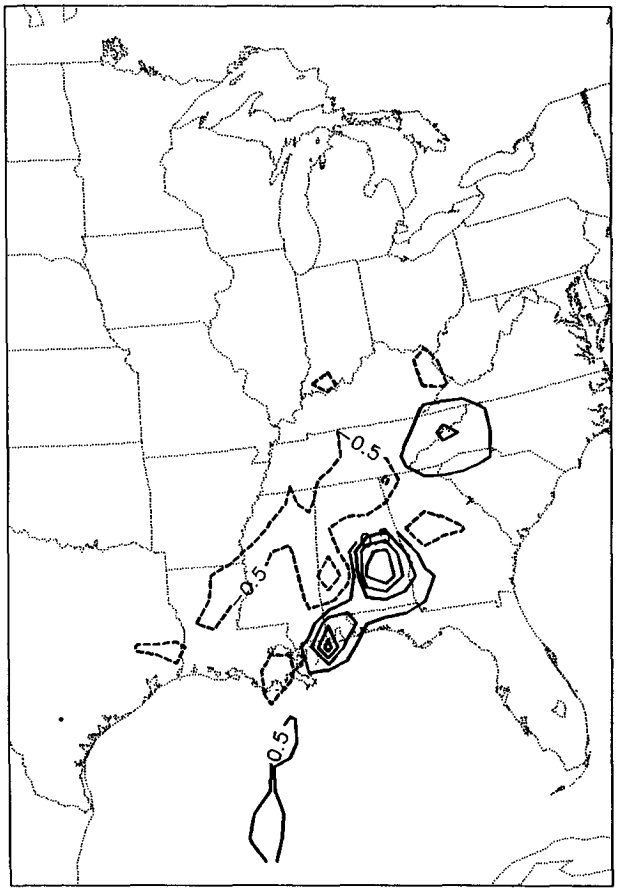

FIG 2. Difference field between the two 36-h precipitation forecasts (cm), obtained by subtracting the result of the standard run from that of the MSS run.

In the 36-h precipitation forecast of the standard run shown in Fig. 1, two major regions of precipitation are apparent. The maximum precipitation in the southern region is 10.0 cm and the maximum precipitation in the northern region is 3.6 cm. The difference between the two 36-h precipitation forecasts (with the standard forecast subtracted from the MSS forecast) is shown in Fig. 2. Clearly, the MSS run produces stronger precipitation in the central mesoscale area of the southern region and the maximum precipitation is increased by 2 cm. Outside the central area, however, relatively weak precipitation is produced by the MSS run. These differences are significant, although larger precipitation forecast errors can be caused by other problems in the current operational prediction models. The hourly rainfall rates averaged over the central mesoscale area (240 km × 240 km) of the southern region are compared in Fig. 3. The rainfall rates start to become significantly different between the two runs as they increase to 0.5 cm h^{-1}. The vertical distribution of the divergence at the center of the above mesoscale area is shown in Fig. 4. As explained earlier, the low-level convergence and vertical motion (not shown) are enhanced by the mass sink due to precipitation.

The differences in the low-level temperature and surface pressure forecasts are also notable as shown in Figs. 5 and 6. Specifically, the northern (or southern)

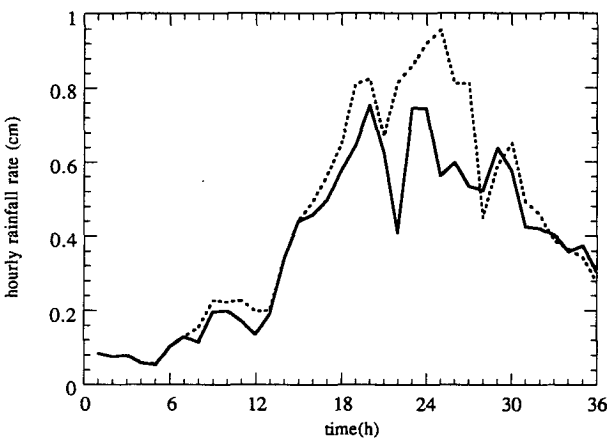

FIG 3. Rainfall rates averaged over the central mesoscale area (240 km × 240 km) in the southern region of maximum precipitation for standard run (solid) and MSS run (dashed).

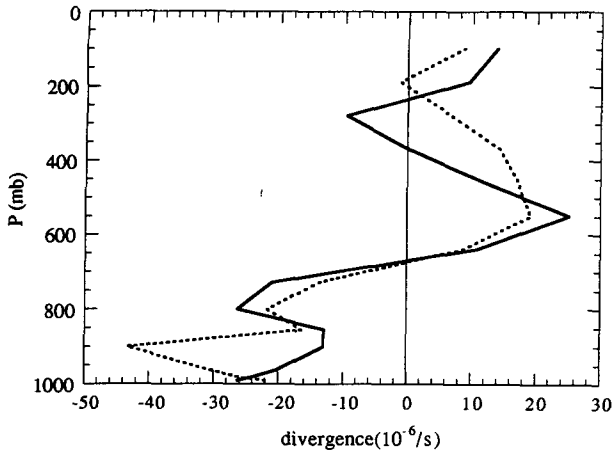

FIG 4. Divergence profiles (solid for standard run and dashed for MSS run) at 36 h in the southern region of maximum precipitation.

part of the cold front moves eastward slightly slower (or faster) in the MSS run than in the standard run. Differences between the 36-h surface pressure forecasts (Fig. 6) are ranged from 3.5 to 1.5 mb. The positive

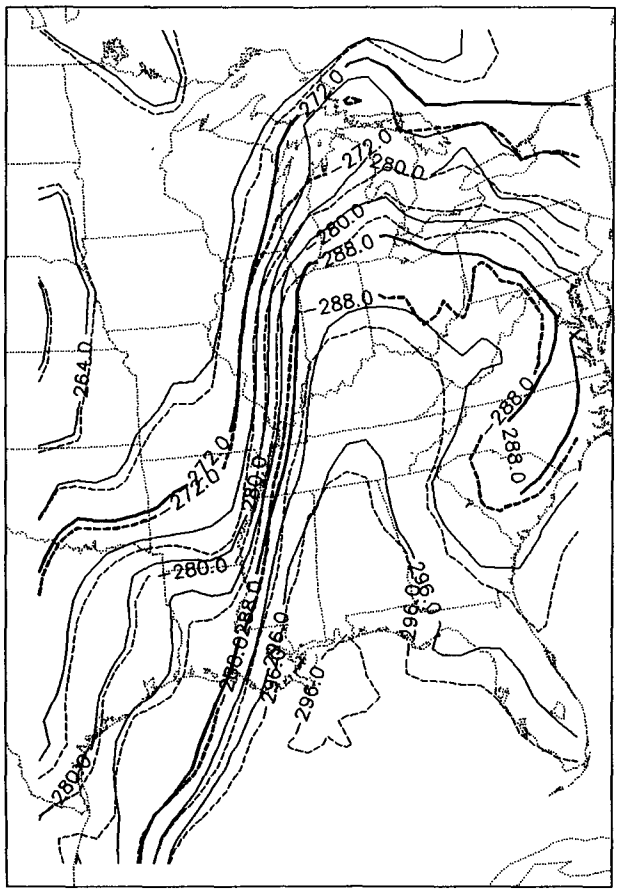

FIG 5. Thirty-six-hour temperature forecasts (K) at $\sigma = 0.97$ by standard run (solid) and MSS run (dashed).

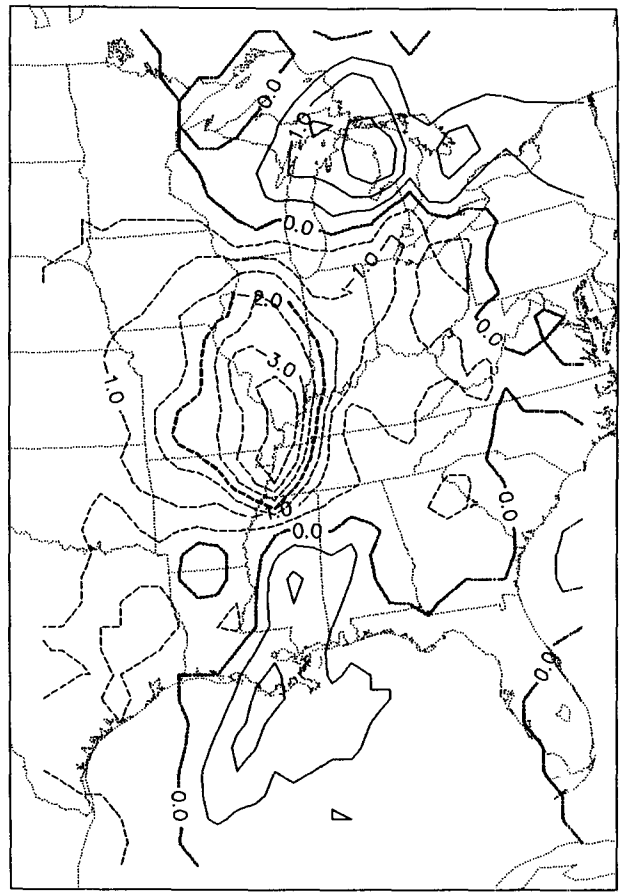

FIG 6. Difference field between the 36-h surface pressure (mb) forecasts, obtained by subtracting the result of the standard run from that of the MSS run.

(negative) areas in the surface pressure difference field correspond roughly to the negative (positive) areas in the low-level temperature difference field (not shown, but may be visually extracted from the two temperature fields in Fig. 5). Clearly, the increase (or decrease) of surface pressure in the MSS run is mainly due to the locally fast (or slow) eastward movement of the cold-frontal zone. Because the surface pressure difference is largely associated with the difference of the positions of the cold front, it is difficult to detect the possible pressure drop caused directly by the mass depletion due to precipitation. Furthermore, the pressure drop caused by the mass depletion may be partially compensated by the tropospheric mass convergence (also caused by the mass depletion) in the precipitation region and may thus be too weak to be detected from the difference field in Fig. 6.

4. Discussion and summary

This study shows that the MSS due to precipitation and evaporation is not always negligible in a numerical model. This supports the results of Gu and Qian (1991)

and is also consistent with the findings of Trenberth et al. (1987), Trenberth (1991), and Van den Dool and Saha (1993). The MSS is real and exists in the atmosphere whenever the water vapor is either depleted from the atmosphere due to condensation and precipitation or added into the atmosphere by evaporation. Our numerical experiments indicate that the MSS terms may not be negligible in numerical simulations of heavy precipitation. When the MSS terms are ignored (as is commonly accepted), the maximum precipitation is likely to be reduced in the model. Since the MSS terms can be easily recovered in the existing numerical models with very little additional computational cost, there seems no reason to neglect the MSS terms. At the very least, the possible importance of the MSS terms in a climate model should be mentioned, as suggested by the studies of Trenberth et al. (1987), Trenberth (1991), and Van den Dool and Saha (1993).

As mentioned earlier, the accuracy of the MSS term in (2.6) depends on the computation of precipitation. Since the numerical simulations presented in this paper have simply assumed that water condensates fall immediately to the ground as soon as they form, the MSS term may not be accurately computed. In particular, the effect of cloud loading (including "drop drag") is ignored. Moreover, because the adjustment time scales back to hydrostatic balance are neglected in all hydrostatic models, the related question is, How significantly does this nonhydrostatic effect influence the density and velocity (relative to air) of water condensate and, thus, affect the accuracy of the MSS term in (2.6)? This question cannot be fully answered until the cloud- and precipitation-related nonhydrostatic dynamical processes and microphysical processes are thoroughly understood. In this sense, this note merely serves to bring up a scientific question with regard to the often-neglected effect of the mass sink due to precipitation.

Acknowledgments. We are grateful to Drs. Alan Shapiro, Huug M. van den Dool, and anonymous reviewers for their interest, comments, and suggestions. The computing resources used in this research are supported by NCAR, which is sponsored by the National Science Foundation. The financial support for this work is provided by the NOAA Contract NA90-RAH00078 and NSF Grants ATM-8822782 and ATM-9113906 at CIMMS, University of Oklahoma.

REFERENCES

Anthes, R. A., E.-Y. Hsie, and Y.-H. Kuo, 1987: Description of the Penn State/NCAR mesoscale model version 4 (MM4). NCAR/TN-282 + STR, National Center for Atmospheric Research, Boulder, CO, 66 pp.

Gu, H., and Z. Qian, 1991: A discussion about the role of the water vapor source/sink term in continuity equation of numerical models. *Chin. Sci. Bull.*, **36**, 16–21.

Trenberth, K. E., 1991: Climate diagnostics from global analyses: Conservation of mass in ECMWF analyses. *J. Climate*, **4**, 707–722.

——, J. R. Christy, and J. G. Olson, 1987: Global atmospheric mass, surface pressure, and water vapor variations. *J. Geophys. Res.*, **92**, 14 815–14 826.

Van den Dool, H. M., and S. Saha, 1993: Seasonal redistribution and conservation of atmospheric mass in a general circulation model. *J. Climate*, **6**, 22–30.